Research article

Kaili Sun, Zongshan Zhao, Yangjian Cai, Uriel Levy and Zhanghua Han*

Ultra-narrowband and highly-directional THz thermal emitters based on the bound state in the continuum

https://doi.org/10.1515/nanoph-2021-0380
Received July 15, 2021; accepted October 8, 2021;
published online October 18, 2021

Abstract: The development of novel and cost-effective THz emitters, with properties superior to current THz sources, is an active and important field of research. In this work, we propose and numerically demonstrate a simple yet effective approach of realizing terahertz sources working in continuous-wave form, by incorporating the new physics of bound state in the continuum (BIC) into thermal emitters. By deliberately designing the structure of slotted disk array made of high-resistivity silicon on top of a low index dielectric buffer layer supported by a conducting substrate, a quasi-BIC mode with ultra-high quality factor (~10^4) can be supported. Our results reveal that the structure can operate as an efficient terahertz thermal emitter with near-unity emissivity and ultranarrow bandwidth. For example, an emitter working at 1.3914 THz with an ultranarrow linewidth less than 130 MHz, which is roughly 4 orders of magnitude smaller than that obtained from a metallic metamaterial-based thermal emitter, is shown. In addition to its high monochromaticity, this novel emitter has additional important advantages including high directionality and linear polarization, which makes it a promising candidate as the new generation of THz sources. It holds a great potential for practical applications where high spectral resolving capability is required.

Keywords: bound state in the continuum; terahertz; thermal emitter.

***Corresponding author: Zhanghua Han**, Shandong Provincial Key Laboratory of Optics and Photonic Devices, Center of Light Manipulation and applications, School of Physics and Electronics, Shandong Normal University, Jinan 250358, China,
E-mail: zhan@sdnu.edu.cn. https://orcid.org/0000-0002-4177-2555
Kaili Sun, Shandong Provincial Key Laboratory of Optics and Photonic Devices, Center of Light Manipulation and applications, School of Physics and Electronics, Shandong Normal University, Jinan 250358, China
Zongshan Zhao, College of Environmental Science and Engineering, Qingdao University, Qingdao 266071, China
Yangjian Cai, Shandong Provincial Key Laboratory of Optics and Photonic Devices, Center of Light Manipulation and applications, School of Physics and Electronics, Shandong Normal University, Jinan 250358, China; and School of Physical Science and Technology, Soochow University, Suzhou 215006, China
Uriel Levy, Department of Applied Physics, The Hebrew University of Jerusalem, Jerusalem, Israel

1 Introduction

Terahertz (THz) technology has aroused widespread interest among researchers and technologists in recent decades because of its unique characteristics such as transient, broadband, coherence, and low energy of THz radiations. The importance of THz technology has gradually emerged as an effective research tool in fundamental sciences of physics [1], chemistry [2], and biology [3] and not of lesser importance as a driving force for the rapid market growth in a vast variety of areas including wireless communications [4], biomedical diagnosis [5], military radar [6], object imaging [7], etc. Although considerable research efforts have been made in this area, the development of THz technology still falls far behind optics or electronics, giving rise to the term 'THz gap'. The bottleneck in this discipline is mainly due to the lack of efficient radiation sources with required characteristics, e.g. sufficient power and acceptable energy efficiency, large bandwidth coverage for pulsed waves or high spectral tunability for continuous-wave (CW) radiations, ease of manufacturing, and economic feasibility. For THz sources working in the CW mode, it is also often required that the output bandwidth is sufficiently narrow. For example, in sensing applications, which is believed to be perhaps the most prominent application of THz technology, a narrow bandwidth of the THz radiation guarantees that the spectral information of the target substance can be properly resolved. This feature is extremely important, particularly for cases where the substance has very fine spectral structures, or if the substance is in a gas state with low concentration and low pressure, presenting an

extremely sharp absorption resonance. To date, many different methods have been used to realize narrowband CW terahertz sources, including free electron lasers (FEL) [8, 9], gas lasers [10], photomixers [11], ultrafast photodiodes [12], and THz quantum cascade lasers (QCL) [13, 14]. However, all these approaches have their respective drawback and limitations. As an example, although FEL and gas lasers can produce large power output with high coherence, they are basically limited mostly to laboratory environments due to their high power consumption, large size, and poor portability. Photomixers and ultrafast photodiodes like unitraveling carrier photodiodes (UTC-PD) [15] rely on the subpicosecond response time of the mobile photocarriers to generate THz radiations and the devices have the advantages of high portability and ease of use. Unfortunately, the output power decreases substantially as the frequency increases, and thus such devices are mostly suitable for frequencies below 1.0 THz. The structure of the QCL is compact and its power consumption is low; however, it typically requires cryogenic working conditions and is still very challenging to operate below 2 THz. Furthermore, the manufacturing of photomixers, photodiodes, and QCLs is based on the III–V semiconductor materials and requires complicated and expensive epitaxy growth techniques. So in this context, the development of compact, cost effective, and efficient THz sources with less technological challenges still needs more research efforts.

A traditional way of generating THz radiations is to use a blackbody thermal emitter. According to Planck's law, thermal emitters generally exhibit a broad spectrum with their emissivity and central frequency determined by the temperature of the emitter. In contrast, one can use artificial resonating structures which exhibit high absorptivity at specific resonance frequencies mainly determined by the structure properties rather than by the temperature. Based on Kirchhoff's law of thermal radiation, the emissivity of an object is the same as its absorptivity in terms of frequency, polarization, and direction. So one can exploit the concept of a perfect absorber typically composed of metallic metamaterials to realize a thermal emitter at the desired frequency range. By carefully designing the structures, one can further minimize the absorption bandwidth to realize relatively narrow band thermal emitters. In recent years, the interest in narrow band thermal radiation sources is mainly concentrated on the midinfrared (MIR) range [16]. Various schemes have been demonstrated to maximize the absorptivity of the emitter at a target frequency while minimizing it at all other frequencies. Examples for such schemes include the use of structures in various forms like plasmonic antennas [17], photonic crystals [18], quantum well structures [19], and metamaterials [20]. Greffet et al. presented a pioneering study, demonstrating that by introducing periodic grating structures into the polar material of SiC, due to the excitation of surface phonon polaritons at the SiC/air interface, the structure supports a directional and narrowband thermal radiation [21]. Zoysa et al. achieved a controlled conversion from a broadband to a narrowband thermal emission spectrum using the photonic crystal resonance effect and quantum well intersubband transition [22]. In addition, S. Fan et al. realized narrowband thermal radiation through the critical coupling between flat tungsten surface and guided resonance in photonic crystals [23, 24]. Another typical structure is the Sandwich configuration, where the structured top metal layer is separated from the bottom reflective surface by a central dielectric spacer. The bottom layer is usually thick enough to prevent any transmission through the structure. The emissivity can be tuned by the thickness of the central spacer layer so that the impedance of the structure matches that of the environment to minimize reflection (equivalently, maximize the emissivity) at resonance. Unfortunately, due to the strong absorption of metals which are the main constituent material for the above structures, the emission peak at the resonance frequency is usually wide with Q values typically at the order of 10. There are also some attempts to use the same idea to realize THz thermal emitters; however, the reported metamaterial-based narrowband thermal THz emitters only possess a bandwidth of about 1 THz at the central frequency in the 4 to 8 THz range [20], restricting their applications in many cases where the high spectral resolving property is required. In general, the exploration of thermal emitters with narrow bandwidth based on new concepts and physics remains an active field. Quite recently, S. Fan et al. also realized narrowband thermal radiations by moiré effect in a twisted two-grating structure above a tungsten substrate, with the corresponding Q-factor as high as 826 [25].

In this work, we propose a novel and cost-effective approach of realizing narrow band THz thermal emitters by combining the thermal emitter with the phenomenon of bound state in the continuum (BIC) [26, 27], which was first investigated in quantum mechanics and was introduced to photonics only in recent years. BIC is typically divided into two groups: symmetry-protected type operating at the Γ point, and the off-Γ accidental type [28], both exhibiting infinite lifetime and quality factor. By introducing a slight perturbation into the BIC structure, the ideal BIC can be tuned into the quasi-BIC mode, with finite yet ultrahigh quality factors and more relieved excitation conditions. Here, we exploit a quasi-BIC mode which is supported by

high-index dielectric material. This high dielectric layer replaces the top metal structure which is typically used in metamaterial-based thermal emitters. Due to the elimination of radiative loss in the quasi-BIC mode and the reduction of metal absorption when the dielectric is used instead of metal, the problem of large bandwidth associated with metal-based thermal emitters can be effectively circumvented. We employ a structure of slotted high index dielectric disk array, which has been investigated recently for applications of nonlinear optics [29]. The air slot is introduced into the disk elements to break the symmetry of the structure, rendering the BIC resonance into a quasi-BIC mode, which can be easily excited by a plane wave of the linear polarization. When this slotted disk array is separated from a conductive reflecting substrate by a lower index spacer layer, it switches to operate in reflection mode, exhibiting a sharp resonance in the reflection spectrum, associated with a high absorptivity at the quasi-BIC mode. According to Kirchhoff's law of thermal radiation, when the same structure is heated to a high temperature, thermal radiation of the same electromagnetic property as the absorptivity will be emitted. Thanks to the high quality factor of the quasi-BIC mode, a THz thermal emitter working in the THz band with a narrow resonance bandwidth can be achieved. We note that although all-dielectric thermal emitters [30] supporting Mie resonances have been proposed in the literature for the purpose of realizing narrow band thermal emitter, our structure proposed in this work further compresses the resonance linewidth by two orders of magnitude. Furthermore, due to the existence of the air slot, the emitted THz radiation has further advantages of linear polarization and high directionality, making this thermal emitter an appealing THz source for many applications.

2 Structure and results

Our proposed thermal emitter with ultranarrow bandwidth is schematically illustrated in Figure 1. High resistivity silicon (HRSi) is assumed as the high index dielectric, for its abundant availability and the full compatibility of the structure manufacturing with the CMOS process, although other dielectric materials with better thermal and electromagnetic performances can also be used. The whole structure is similar to the Sandwich configuration widely adopted for metallic metamaterial-based thermal emitter [31], except that the top metal layer is replaced by an array of HRSi disks. The yellow region denotes the reflective metallic substrate, which is assumed to be made of copper (conductivity 5.8×10^7 S/m). By applying direct current (DC), the substrate can be heated to a certain temperature, resulting in an upward THz emission, as illustrated by Figure 1(a). We first use the experimentally measured values of refractive index and absorption in the THz band at room temperature for the HRSi material (the index is adopted to be constantly 3.418, and the imaginary part of the refractive index is 7.162×10^{-5}, which corresponds to an absorption coefficient of 0.03 cm^{-1} around 1.0 THz [32]). The disk array having the same periodicity P = 120 μm along both directions is separated from the substrate by a spacer layer of lower refractive index (1.5) and height h = 10 μm. The disks are assumed to have a radius R = 32 μm and thickness T = 40 μm, respectively. An air slot with length L = 10 μm and width W = 4 μm is etched through the disk layer, with its center shifted by a distance D = 2 μm relative to that of the HRSi disks. These geometrical parameters are assumed constant throughout this paper. The presence of the air slot makes the quasi-BIC mode easily excited by a linearly polarized plane wave [33]. In the context of the thermal emitters, it means that the emitted radiation from the same structure will reciprocally have the same planar wave-front distribution and polarization property.

The dispersion properties of the resonances supported by the structure are investigated using the finite element method (FEM) implemented in the commercial software of COMSOL Multiphysics. Floquet periodic boundary conditions are applied in the xy plane while perfectly matched layers are used along the z direction. The band structure of

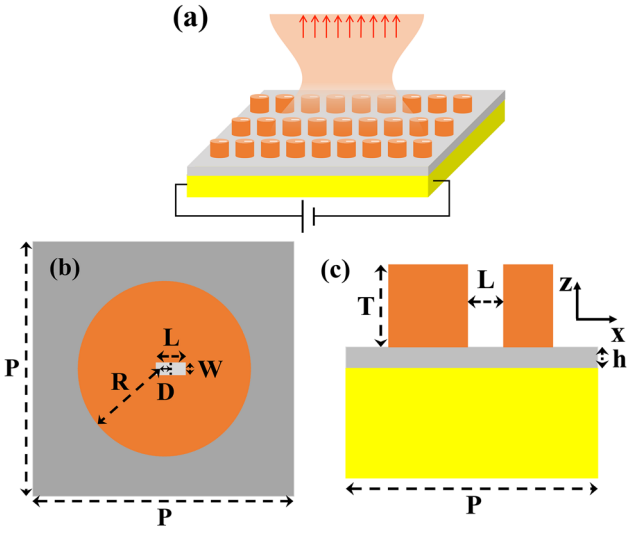

Figure 1: (a) The schematic diagram of the ultra-narrow bandwidth THz thermal emitter, assisted by the BIC mode supported by the Si slotted disk array; the orange output beam represents the thermal emission at the BIC resonance. (b) and (c) Top and cross-sectional views of Si slotted disk array unit cell, respectively.

the resonance supported by the slotted disk array is plotted as the solid blue curves in Figure 2(a), whereas the dashed lines mark the light dispersion in air. The cone region above the light lines is the so called radiation continuum and one can see that the resonance supported by the HRSi slotted disk array falls well within this region. As shown in Figure 2(b), both the eigen frequency and the associated quality factor (Q-factor) are slightly affected by the lateral wave vector. At a zero lateral wave vector, a higher Q-factor of above 1.11×10^4 is achieved. As the wave vector increases, the frequency decreases with a slight drop of the Q-factor. However, the overall Q-factor is always above 9×10^3. The result suggests that no matter a normal or slightly inclined incidence is applied, a reflection resonance with a high Q-factor can be obtained. These values are significantly higher than that can be achieved with traditional metal thermal emitters [34] or all-dielectric thermal emitters [30]. Note that the Q-factor supported by the slotted HRSi disk array can in general be further manipulated by the degree of asymmetry of the whole system, i.e. by the dimension and position of the air slot [29]. For example, when D reduces from 2 to 1 μm, the calculated Q-factor at a lateral wave vector increase from 1.11×10^4 to 1.72×10^4. The dependence of the quasi-BIC resonance frequency on the lateral wave vector also implies that for the investigated structure, when the incidence angle changes, the frequency of the quasi-BIC resonance will experience a shift. Correspondingly, when the structure works as a thermal emitter, the emitted radiations will spread out at different outward inclination angles for different frequencies.

The emission characteristics of the structure are further studied numerically. According to Kirchhoff's thermal emission law [35], for any object that emits and absorbs thermal emission in a thermodynamic equilibrium state, its emissivity is equal to the absorptivity. So the emissivity $E(\omega)$, which is defined as the emission of an object normalized to that of a blackbody, can be characterized by the absorptivity $A(\omega) = 1 - T(\omega) - R(\omega)$, where $T(\omega)$ and $R(\omega)$ are transmissivity through and reflectivity from the entire structure, respectively. Because the substrate is opaque and the transmissivity is always 0, the absorptivity as well as the emissivity can be simply expressed as $E(\omega) = A(\omega) = 1 - R(\omega)$. Therefore, one only needs to investigate the absorbing property of the structure at different excitations instead, and the obtained results will represent the emission properties. This approach has been widely used in the investigation of metamaterial-based thermal emitters.

The solid line in Figure 3(a) presents the calculated absorptivity/emissivity at room temperature for the slotted Si disk array with the geometrical parameters described above. The calculation assumes normally incidence, linearly polarized along the y direction plane wave excitation. Due to the reciprocal property between absorption and emission processes, the radiation from the proposed thermal emitter will have the same property as the incident light used in the calculations. The results in Figure 3(a) show that the emissivity at resonance reaches 1.0 and the emission bandwidth is around 125 MHz at the resonance frequency of 1.3914 THz. The latter two values correspond to a Q-factor of 1.11×10^4, which is consistent with the

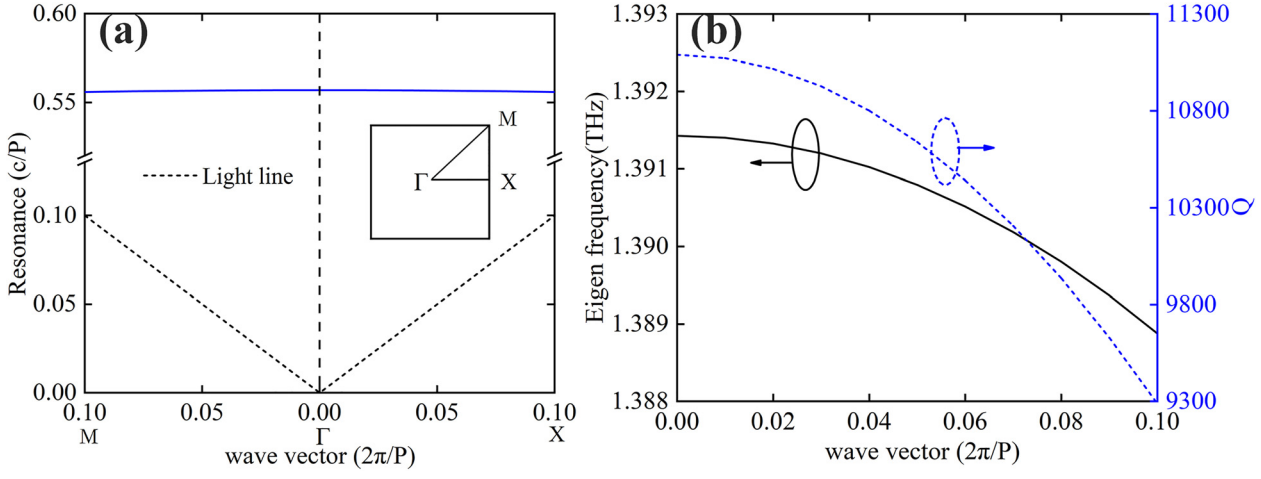

Figure 2: (a) The band structure of the BIC mode supported by the slotted HRSi disk array. The blue line represents the BIC mode, while the dashed lines mark the light dispersion. (b) Resonance eigen frequencies and the associated Q-factors of the BIC mode as a function of the lateral wave vector.

results presented in Figure 2(b). We note that a bandwidth of about 100 MHz is roughly 4 orders of magnitude smaller than that achieved by metal metamaterial-based thermal THz emitters [20]. To reveal the underlying physics of the quasi-BIC resonance supported by this structure, we further plot in Figure 3(c) the top view of the magnetic field magnitude as well as the vectorial distribution of the electric field at resonance across the central plane of the Si disk. The result resembles that of a quasi-BIC mode supported by similar slotted disk array made of high index dielectrics but on a low index substrate [29]. The magnetic field distribution in Figure 3(d) shows that the field of the quasi-BIC mode is indeed concentrated in the top Si layer, in contrast to the case of metamaterial-based thermal emitters where the field is compressed to the central spacer between two metallic layers.

We note that the BIC mode supported by the bare Si disk array cannot be excited by a plane wave due to a zero field overlap between the incident plane wave and the BIC mode (dark mode). However, when the air slot is present, it works as a void antenna and will be first activated by the plane wave, followed by a subsequent excitation of the azimuthally polarized quasi-BIC mode. So for the reverse process of thermal emitting, we believe the circularly distributed electric displacement current will be first generated inside the Si disk array. The displacement current will be further coupled by the air slot into the vacuum as an upwardly propagating plane wave. The strength of both processes will become stronger as the temperature increases. As one can see from the inset of Figure 3(a), there is a single emission line in the 1.0–1.5 THz for the *y*-polarization. For the cross-polarization (i.e. the *x*-polarization), it is also quite far away from 1.3914 THz. This is because for the *x*/*y* polarization, it corresponds to the longer/shorter side of the air slot, respectively [36]. As a result, the resonance will see a significant blue-shift when

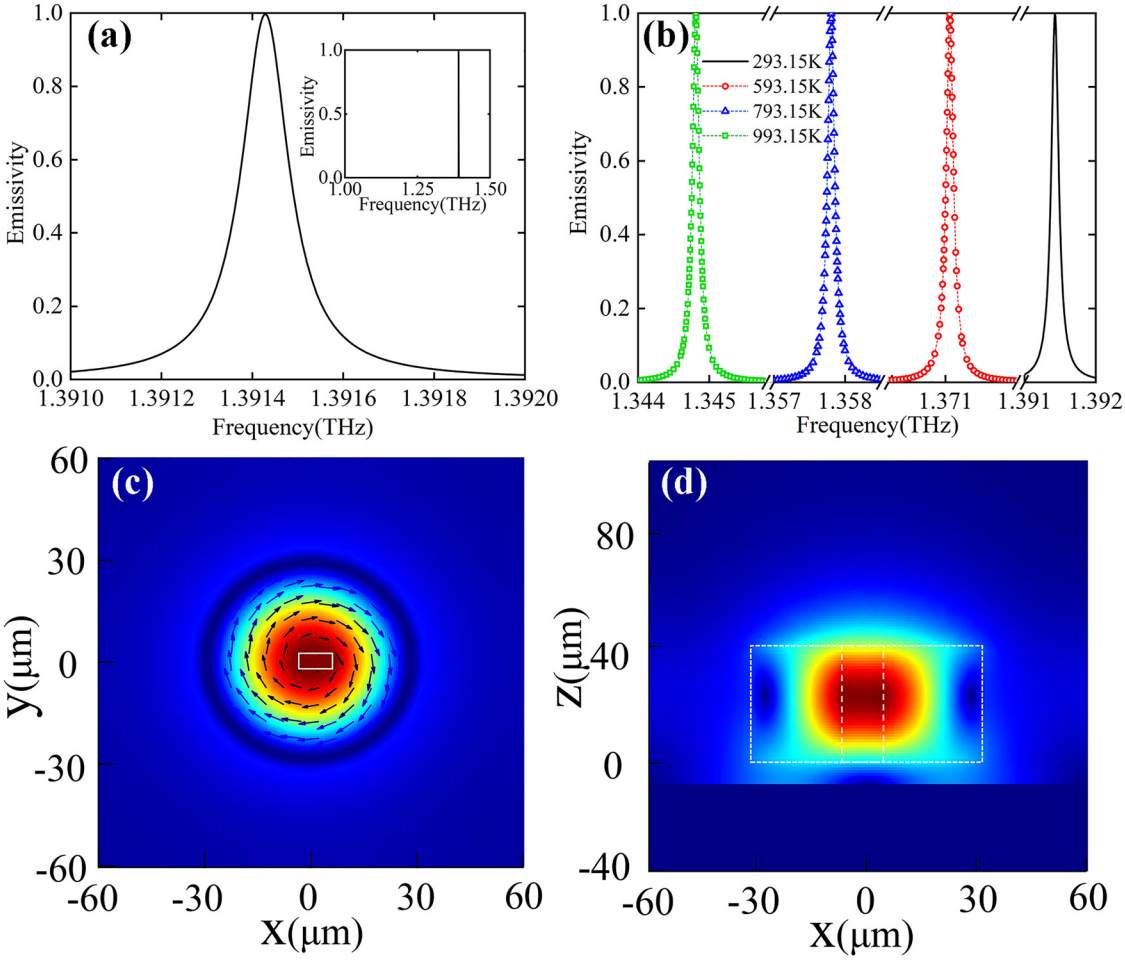

Figure 3: (a) Normalized emission spectrum of the slotted Si disk array at normal direction and *y*-polarization; the inset shows the narrow spectral response of the device in a broader bandwidth scale (1.0–1.5 THz); (b) emission spectra at different temperatures by fully taking into account the thermal influence to the properties of HRSi. The red circle, blue triangles and green squares represents the emissivity calculated at 593.15, 793.15, and 993.15 K; (c) top view of the magnetic field and electric field vectorial distribution at resonance across the central plane of the Si disk array. (d) The *xz* cross-sectional view of the magnetic field amplitude distribution at resonance.

the polarization switches from y to x. The single emission line and the high spectral purity is an asset of the thermal emitter, because it eliminates the requirement of complicated narrow-band filters to extract the emitted signals.

The above results are obtained by assuming the HRSi index to be constant $n_{RT} = 3.418 + 7.162 \times 10^{-5}$ j in the spectral range of our interest. For thermal emitters whose structure will be heated to high temperatures, two typical effects will have to be considered which will significantly influence the HRSi permittivity and the emission property. One is the thermo-optic effect, which will lead to a considerable change of the refractive index at different temperatures. The other is the thermally excited free carrier effect exclusively for semiconductor materials, and the excited carriers will result in a dispersion and additional loss, which must be considered. To get more insight into this issue, we use the complex model in Eq. (1) to characterize the complex dielectric constant of silicon:

$$\epsilon(\omega, T) = (n_{RT} + \beta\Delta T)^2 - \frac{\omega_p(T)^2}{\omega^2 + j\omega\gamma(T)} \quad (1)$$

where β is the thermo-optic coefficient, $\omega_p(T)$ is the plasma frequency and is related with the free carrier density $n(T)$ as:

$$\omega_p^2 = \frac{e^2 n(T)}{\epsilon_0 m^*} \quad (2)$$

We adopted the value measured at 1550 nm as 1.8×10^{-4}/K [37] for further calculations, which is very close to the experimentally measured thermo-optic efficient of HRSi at 659 GHz [38]. The discrepancy between the real value of it at THz band to 1.8×10^{-4}/K may lead to a spectral shift of the calculated spectrum, but doesn't affect our conclusions. The damping factor $\gamma(T)$ in Eq. (1) characterizes the collision rate between free carriers and crystal lattice and is reflected in the carrier mobility $\mu(T)$ by $\gamma(T) = e/(m^*\mu(T))$ where e and $m^* = 0.26m_0$ (m_0 is the static mass for electrons) are the electron charge and effective mass, respectively. For the thermally excited free carriers in intrinsic silicon, the concentration $n(T)$ is relatively low, so the mobility model for lightly doped silicon as a function of temperature is used as $\mu(T) = 8.56 \times 10^8 \times T^{-2.33}$ [37]. Combining the dependence of free carrier density for intrinsic semiconductor, $n(T) = n_0 \exp(-E_g/2k_0T)$ where k_0 is the Boltzmann's Constant, n_0 is set as 3.8325×10^{19} cm^{-3} which will lead to a typical intrinsic carrier density for silicon at 300 K as 1.5×10^{10} cm^{-3}, one can calculate using Eq. (1) the complex permittivity for silicon at a certain temperature. Using this model, we recalculate the emission spectrum at a high temperature of 593.15, 793.15, and 993.15 K, the results are presented as the dashed line marked with circles, triangles and squares in Figure 3(a). One can see a substantial red shift when the temperature increases, and the shift is mainly attributed to the refractive index change of silicon due to thermo-optic effect. For the contribution from the free carrier effect at high temperatures, our calculations show that the real part of silicon permittivity changes only by an order of 10^{-4} at around 1.3914 THz at the temperature of a few hundred Kelvin, which, however, will induce a much smaller spectral shift compared to the thermo-optic effect. One can also see in Figure 3(b) that both the emissivity and the bandwidth (still less than 130 MHz) remain almost unchanged at 593.15, 793.15 and 993.15 K. That is because the thermal carriers will introduce negligible loss to silicon at this temperature. The imaginary part change of silicon permittivity is found to be at the order of 10^{-7} in this spectral range. All those results demonstrate that the increase of temperature will provide an additional means of fine tuning of the emission frequency, while it is not so detrimental to the performance of the emitters.

Besides the ultranarrow bandwidth and the simple linear polarization properties of the proposed thermal emitter, another important property of a source is its beam directionality. To study this feature, we calculated the emission pattern at four different frequencies of 1.3914, 1.3913, 1.3891, and 1.3820 THz. The calculation is achieved using the same method based on Kirchhoff's law by calculating the reflection spectrum at different incident angles for a specific frequency. The incidence plane coincides with the xz plane and the inclination angle is relative to the z axis. The calculated emissivity/absorptivity patterns are presented in Figure 4(a). To clearly present that angular dependence of the emissivity, we also plot in Figure 4(b) an enlarged version in a small angular range for the frequency of 1.3914 THz. One can see that for this frequency, the emissivity exhibits a sharp decrease from 1.0 at normal incidence to almost 0 when the incident angle increases to 5°. The angular full-width at half-maximum (FWHM) is only around 3°, indicating a highly directional property of the output beam. We also calculated the angle-dependent emission as a function of output angle in the 3D space. The results demonstrate that the output THz radiation at 1.3914 THz is almost normal to the top surface of the thermal emitter, regardless of whether the output angle is along x or y direction. This property is consistent with the result given in Figure 2(a) that the eigen frequency is not barely affected by the wave vector being along either ΓX or ΓM direction.

For other frequencies different from 1.3914 THz, one can see in Figure 4(a) that the emission is along two directions symmetric with the structure normal. Actually in

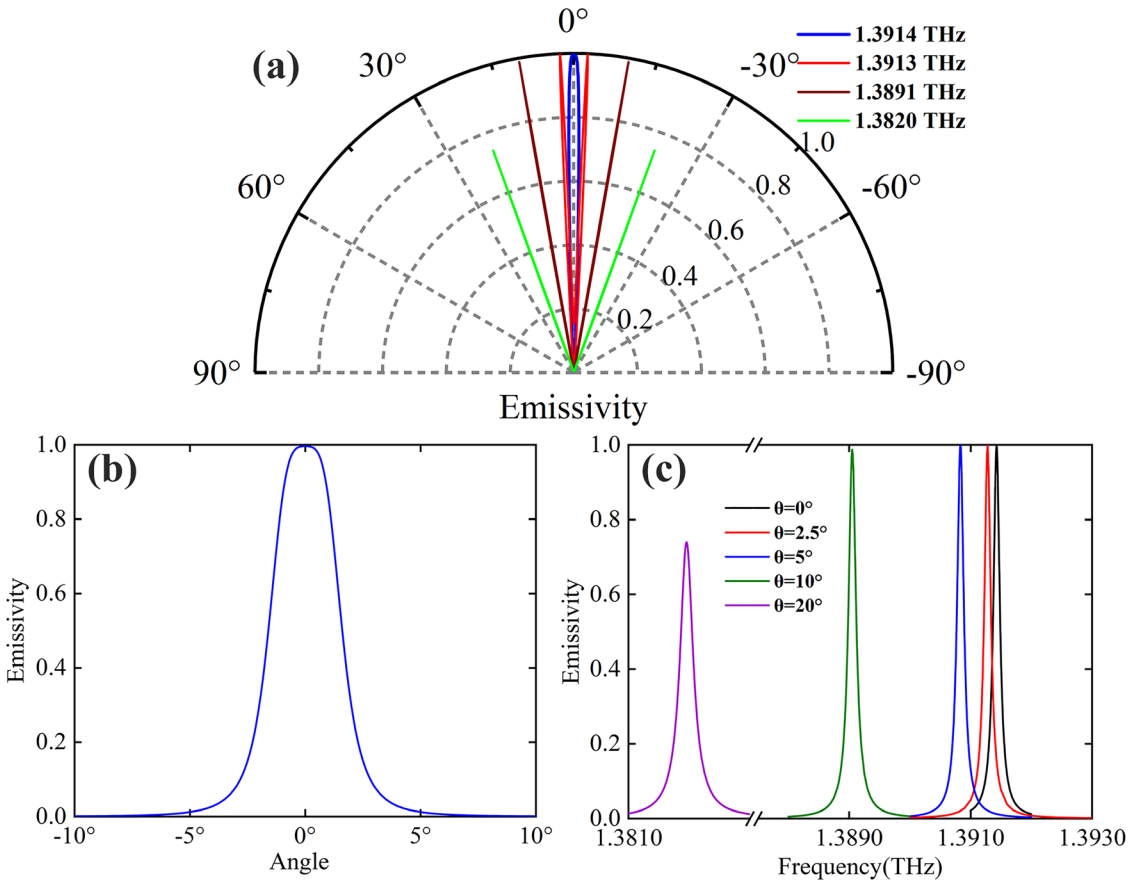

Figure 4: (a) Polar plot of the emissivity for four different emission frequencies of 1.3914, 1.3913, 1.3891 and 1.3820 THz; (b) An enlarged view of (a) at 1.3914 THz; (c) the emission frequency spectrum at different incident angles (θ = 0°, 2.5°, 5°, 10°, and 20°).

the 3D space, the emission patterns have a cone shape. As the frequency deviates further from 1.3914 THz, the cone angle increases and the emissivity also experiences a slight decrease. In Figure 4(c) we plot the emission spectrum of the proposed thermal emitter as a function of the emission angle in the *xz* plane. One can see that there is a specific emission frequency for a certain emission direction, e.g. 1.3913 THz for 2.5°, 1.3891 THz for 10°, and 1.3820 THz for 20°. The results in Figure 4(a) and (c) show that when the thermal emitter is heated, it actually emits radiations with different frequencies. This kind of 'rainbow' characteristics, i.e. light emission at different wavelengths being radiated toward different directions, is consistent with other types of nanophotonic engineered thermal emitters [38]. Each frequency is spread out along different output angle and the emissivity also sees a decrease at larger output angles. For a fixed structure geometry, there is a characteristic frequency (1.3914 THz here) at which the emission is normal to the structure surface with the highest emissivity. The radiations at this frequency will be mostly exploited because it will eliminate the necessity of other components like Si sphere lenses to achieve highly collimated THz beams. However, other frequencies can also be used by applying a spatial frequency filter to extract the THz signals with frequency of interest.

3 Discussions and conclusion

Note that in all the above calculations, HRSi is used as the high index material due to its abundant availability and the high compatibility of the structure fabrication with CMOS technology. So the thermal properties including both the thermo-optic and free carrier effects and their influence to the HRSi permittivity must be considered. In real-world applications, one may need to realize a thermal emitter at a specific frequency, e.g. to match the absorption resonance of a target chemical. The first approach one can consider to tune the emission frequency is to scale the geometry of the structure. Since the HRSi index and absorption remains

almost the same between 0.1 and 2.0 THz [32], one can expect the same emission property within this range. In addition to geometrical changes of the structure, which will result in a substantial shift of the emission resonance, one can also make use of the dependence of silicon permittivity in the THz band due to the two thermal effects. Even when the refractive change is weak, a spectral shift can still be expected considering the ultranarrow bandwidth of the emission resonance. This provides one additional degree of freedom to achieve a fine tuning of the emission frequency, with no significant degrading of the emitter performances. On the other hand, other high index refractory dielectrics like ceramics or silicon carbide, which has less influence by the thermal effects, can be used instead of HRSi.

In summary, in this paper we have introduced a completely new yet efficient approach of realizing thermal emitters, by replacing the top layer of metallic structures in the Sandwich configuration of metamaterial-based thermal emitters with high-index dielectric structures. The dielectric structure array supports a quasi-BIC mode, which has unprecedented high Q-factor and can help to realize thermal emission with ultranarrow output bandwidth. We have numerically demonstrated a THz thermal emitter working at 1.3914 THz with an output bandwidth of the order of 100 MHz, by using a slotted Si disk array to support the BIC mode. Besides the high monochromaticity, our proposed structure possesses additional advantages such as linear polarization, high directionality, and the possibility of extracting THz radiation at slightly different frequencies by using spatial frequency filters. One can also change the Si disk array geometry to tune its resonance so that CW form of radiation at frequencies covering the whole THz band can be realized. The emissivity at different frequencies can be optimized by changing the spacer layer thickness, so the deficiency of power decaying at the increase of output frequency associated with semiconductor based THz sources can be circumvented. Furthermore, this scheme requires only a high index dielectric in the THz band like the most abundant material of Si employed in this work, eliminating the requirement of expensive III–V materials. With all these superior properties, our BIC enhanced thermal emitter represents a good candidate to realize efficient THz sources, and may strongly mitigate the bottleneck problem in THz sciences. Furthermore, the idea can be pushed forward towards even higher frequencies in the mid-infrared, laying out the foundation for sensing applications in a broad spectral range.

Author contribution: All the authors have accepted responsibility for the entire content of this submitted manuscript and approved submission.

Research funding: National Natural Science Foundation of China (11974221, 11974218, 91750201) and Local science and technology development project of the central government of China (No. YDZX20203700001766).

Conflict of interest statement: The authors declare no conflicts of interests.

References

[1] X. Wang, H. Meng, S. Deng, et al., "Hybrid metal graphene-based tunable plasmon-induced transparency in terahertz metasurface," *Nanomaterials*, vol. 9, no. 3, p. 385, 2019.

[2] J. F. Federici, B. Schulkin, F. Huang, et al., "THz imaging and sensing for security applications – explosives, weapons and drugs," *Semicond. Sci. Technol.*, vol. 20, no. 7, pp. S266–S280, 2005.

[3] G. Sancho-Fornes, M. Avella-Oliver, J. Carrascosa, E. Fernandez, E. M. Brun, and Á. Maquieira, "Disk-based one-dimensional photonic crystal slabs for label-free immunosensing," *Biosens. Bioelectron.*, vol. 126, pp. 315–323, 2019.

[4] A. J. Seeds, H. Shams, M. J. Fice, and C. C. Renaud, "TeraHertz photonics for wireless communications," *J. Lightwave Technol.*, vol. 33, no. 3, pp. 579–587, 2015.

[5] X. Yang, X. Zhao, K. Yang, et al., "Biomedical applications of terahertz spectroscopy and imaging," *Trends Biotechnol.*, vol. 34, no. 10, pp. 810–824, 2016.

[6] S. Ergün and S. Sönmez, "Terahertz technology for military applications," *J. Mil. Inf. Sci.*, vol. 3, no. 1, p. 13, 2015.

[7] B. B. Hu and M. C. Nuss, "Imaging with terahertz waves," *Opt. Lett.*, vol. 20, no. 16, p. 1716, 1995.

[8] P. Tan, J. Huang, K. F. Liu, Y. Q. Xiong, and M. W. Fan, "Terahertz radiation sources based on free electron lasers and their applications," *Sci. China Inf. Sci.*, vol. 55, no. 1, pp. 1–15, 2012.

[9] N. Vinokurov, "Free electron lasers as a high-power terahertz sources," *J. Infrared, Millim. Terahertz Waves*, vol. 32, no. 10, pp. 1123–1143, 2011.

[10] P. Chevalier, A. Amirzhan, F. Wang, et al., "Widely tunable compact terahertz gas lasers," *Science*, vol. 366, no. 6467, pp. 856–860, 2019.

[11] H. Tanoto, J. H. Teng, Q. Y. Wu, et al., "Nano-antenna in a photoconductive photomixer for highly efficient continuous wave terahertz emission," *Sci. Rep.*, vol. 3, no. 1, p. 2824, 2013.

[12] T. Nagatsuma, H. Ito, and T. Ishibashi, "High-power RF photodiodes and their applications," *Laser Photon. Rev.*, vol. 3, nos 1–2, pp. 123–137, 2009.

[13] G. Davies and E. Linfield, "Invited – terahertz quantum cascade lasers," *IEEE MTT-S Int. Microw. Symp. Dig.*, vol. 2, pp. 743–746, 2003.

[14] Y. Yao, A. J. Hoffman, and C. F. Gmachl, "Mid-infrared quantum cascade lasers," *Nat. Photonics*, vol. 6, no. 7, pp. 432–439, 2012.

[15] H. Ito, F. Nakajima, T. Furuta, and T. Ishibashi, "Continuous THz-wave generation using antenna-integrated uni-travelling-carrier photodiodes," *Semicond. Sci. Technol.*, vol. 20, no. 7, pp. S191, 2005.
[16] T. Inoue, M. De Zoysa, T. Asano, and S. Noda, "Realization of narrowband thermal emission with optical nanostructures," *Optica*, vol. 2, no. 1, p. 27, 2015.
[17] C.-M. Wang and D.-Y. Feng, "Omnidirectional thermal emitter based on plasmonic nanoantenna arrays," *Opt. Express*, vol. 22, no. 2, p. 1313, 2014.
[18] B. J. O'Regan, Y. Wang, and T. F. Krauss, "Silicon photonic crystal thermal emitter at near-infrared wavelengths," *Sci. Rep.*, vol. 5, no. 1, p. 13415, 2015.
[19] T. Inoue, M. De Zoysa, T. Asano, and S. Noda, "Wavelength-switchable mid-infrared narrowband thermal emitters based on quantumwells and photonic crystals," *IEICE Trans. Electron.*, vol. E101, no. C7, pp. 545–552, 2018.
[20] F. Alves, B. Kearney, D. Grbovic, and G. Karunasiri, "Narrowband terahertz emitters using metamaterial films," *Opt. Express*, vol. 20, no. 19, p. 21025, 2012.
[21] J.-J. Greffet, R. Carminati, K. Joulain, J.-P. Mulet, S. Mainguy, and Y. Chen, "Coherent emission of light by thermal sources," *Nature*, vol. 416, no. 6876, pp. 61–64, 2002.
[22] M. De Zoysa, T. Asano, K. Mochizuki, A. Oskooi, T. Inoue, and S. Noda, "Conversion of broadband to narrowband thermal emission through energy recycling," *Nat. Photonics*, vol. 6, no. 8, pp. 535–539, 2012.
[23] Y. Guo and S. Fan, "Narrowband thermal emission from a uniform tungsten surface critically coupled with a photonic crystal guided resonance," *Opt. Express*, vol. 24, no. 26, p. 29896, 2016.
[24] W. Li and S. Fan, "Nanophotonic control of thermal radiation for energy applications [Invited]," *Opt. Express*, vol. 26, no. 12, p. 15995, 2018.
[25] C. Guo, Y. Guo, B. Lou, and S. Fan, "Wide wavelength-tunable narrow-band thermal radiation from moiré patterns," *Appl. Phys. Lett.*, vol. 118, no. 13, p. 131111, 2021.
[26] C. W. Hsu, B. Zhen, A. D. Stone, J. D. Joannopoulos, and M. Soljacic, "Bound states in the continuum," *Nat. Rev. Mater.*, vol. 1, no. 9, p. 16048, 2016.
[27] K. Koshelev, A. Bogdanov, and Y. Kivshar, "Meta-optics and bound states in the continuum," *Sci. Bull.*, vol. 64, no. 12, pp. 836–842, 2019.
[28] S. I. Azzam, V. M. Shalaev, A. Boltasseva, and A. V. Kildishev, "Formation of bound states in the continuum in hybrid plasmonic-photonic systems," *Phys. Rev. Lett.*, vol. 121, no. 25, p. 253901, 2018.
[29] Z. Han, F. Ding, Y. Cai, and U. Levy, "Significantly enhanced second-harmonic generations with all-dielectric antenna array working in the quasi-bound states in the continuum and excited by linearly polarized plane waves," *Nanophotonics*, vol. 10, no. 3, pp. 1189–1196, 2021.
[30] M. O. Ali, N. Tait, and S. Gupta, "High-Q all-dielectric thermal emitters for mid-infrared gas-sensing applications," *J. Opt. Soc. Am. A*, vol. 35, no. 1, p. 119, 2018.
[31] X. Liu, T. Tyler, T. Starr, A. F. Starr, N. M. Jokerst, and W. J. Padilla, "Taming the blackbody with infrared metamaterials as selective thermal emitters," *Phys. Rev. Lett.*, vol. 107, no. 4, p. 045901, 2011.
[32] D. Grischkowsky, S. Keiding, M. van Exter, and C. Fattinger, "Far-infrared time-domain spectroscopy with terahertz beams of dielectrics and semiconductors," *J. Opt. Soc. Am. B*, vol. 7, no. 10, p. 2006, 1990.
[33] Z. Han and Y. Cai, "All-optical self-switching with ultralow incident laser intensity assisted by a bound state in the continuum," *Opt. Lett.*, vol. 46, no. 3, p. 524, 2021.
[34] Z. Yang, S. Ishii, T. Yokoyama, et al., "Tamm plasmon selective thermal emitters," *Opt. Lett.*, vol. 41, no. 19, p. 4453, 2016.
[35] G. Kirchhoff, "I. On the relation between the radiating and absorbing powers of different bodies for light and heat," *London, Edinburgh, Dublin Philos. Mag. J. Sci.*, vol. 20, no. 130, pp. 1–21, 1860.
[36] Z. Han, H. Jiang, Z. Tan, J. Cao, and Y. Cai, "Symmetry-broken silicon disk array as an efficient terahertz switch working with ultra-low optical pump power," *Chin. Phys. B*, vol. 29, no. 8, p. 084209, 2020.
[37] N. D. Arora, J. R. Hauser, and D. J. Roulston, "Electron and hole mobilities in silicon as a function of concentration and temperature," *IEEE Trans. Electron. Dev.*, vol. 29, no. 2, pp. 292–295, 1982.
[38] D. G. Baranov, Y. Xiao, I. A. Nechepurenko, A. Krasnok, A. Alù, and M. A. Kats, "Nanophotonic engineering of far-field thermal emitters," *Nat. Mater.*, vol. 18, no. 9, pp. 920–930, 2019.